J|A|C|S
ARTICLES
Published on Web 12/31/2003

Peralkylated Coronenes via Regiospecific Hydrogenation of Hexa-*peri*-hexabenzocoronenes

Mark D. Watson,*[,†,§] Michael G. Debije,[‡] John M. Warman,[‡] and Klaus Müllen*[,†]

Contribution from the Max-Planck-Institute for Polymer Research, Postfach 3148, D-55021 Mainz, Germany, and Interfaculty Reactor Institute (IRI), Delft University of Technology, Mekelweg 15, 2629 JB Delft, The Netherlands

Received July 24, 2003; E-mail: muellen@mpip-mainz.mpg.de; mdwatson@uky.edu

Abstract: A remarkable, regiospecific hydrogenation zips around the ~4 nm perimeter of hexa-*peri*-hexabenzocoronenes (HBC) adding 18 hydrogen atoms, leading to the first peralkylated coronenes, in quantitative yields in some cases. Increasing steric bulk of side chains was found to hinder the reaction, while unsubstituted HBC could be converted to a modest extent despite its vanishing solubility. The structures of the novel coronenes are unequivocally confirmed by MALDI-TOF, ^{1}H, ^{13}C, and heteronuclear correlation NMR, and UV−vis absorption spectroscopy. The puckered-ring periphery of these discotics does not prohibit self-assembly to columnar structures in a fashion similar to that of the planar precursors, as determined from wide-angle X-ray diffraction, but decreases the isotropization temperature by ~300 °C relative to the latter. Branching in the alkyl chains frustrates nucleation from the melt, resulting in clear polymorphism depending on the thermal treatment. Nonetheless, preliminary measurements indicate high charge-carrier mobilities and lifetimes within the bulk material, on the same order as those previously found for HBCs.

Introduction

Catalytic hydrogenation of aromatic hydrocarbons has historically been an unpredictable and uncontrollable undertaking.[1] In some cases, control over site selectivity may be induced through the appropriate choice of reaction conditions including the transition metal[2] and even the purity of that metal.[3] In the area of homogeneous hydrogenations, advances toward selective hydrogenation have been accomplished through the use of diborane catalysts[4] and appropriately substituted cobalt complexes.[5]

We chose to investigate the hydrogenation of hexa-*peri*-hexabenzocoronenes (HBCs, **1**) belonging to the class of all-benzenoid polycyclic aromatic hydrocarbons (PAHs). These are fully delocalized π-systems in which all rings are considered either "full" with an aromatic sextet of π electrons or "empty" as depicted in Scheme 1.[6] It was of interest to assess their susceptibility to hydrogenation and any associated regioselectivity. We report here that exposure of HBCs to moderate hydrogen pressure, in the presence of palladium on activated carbon as catalyst, results in quantitative, regiospecific conversion of suitably substituted HBCs to the first recorded peralkylated coronenes (Scheme 1).[7] Further, the self-assembly of two derivatives to ordered thermotropic discotic columnar structures is demonstrated by thermal, optical, and diffraction methods. Their properties observed to date, including high charge-carrier mobilities as assessed by pulse radiolysis-time-resolved microwave conductivity (PR-TRMC), qualify these materials as promising candidates as active components in organic electronics.

Scheme 1. Hydrogenation of Hexa-*peri*-hexabenzocoronenes

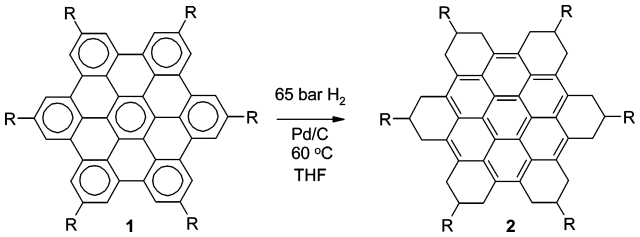

Results

Synthesis and Spectral Characterization. HBC derivatives carrying various substituents were combined with Pd/C (10%) in dry THF, pressurized to 55−65 bar H_2, and heated to 60 °C. Isolated yields and reaction times are collected in Table 1. All compounds were received as pale yellow (semi)crystalline powders, with the exception of **2e**, which was isolated as a pale yellow wax. *n*-Alkyl derivatives **2b**,**c** were obtained in analytically pure form after filtration of the catalyst and solvent evaporation. Unsubstituted derivative **2a** was obtained in pure form after washing the Pd/C with hot *o*-dichlorobenzene, and

[†] Max-Planck-Institute for Polymer Research.
[‡] Delft University of Technology.
[§] New address: Department Chemistry, University of Kentucky, Lexington, KY 40506-0055.

(1) Donohoe, T. J.; Garg, R.; Stevenson, C. A. *Tetrahedron: Assymetry* **1996**, *7*, 317.
(2) Rothwell, I. *Chem. Commun*. **1997** 1331−38.
(3) Harvey, R. J. *Polycyclic Aromatic Hydrocarbons*; VCH: New York, 1997; Chapter 4.
(4) Yalpani, M.; Köster, R. *Chem. Ber*. **1990**, *123*, 719−24.
(5) *Applied Homogeneous Catalysis with Organometallic Compounds*; Cornills, B., Herrmann, W. A., Eds.; VCH: New York, 1996; Vol. 1.
(6) Clar, E. *The Aromatic Sextet*; John Wiley and Sons: London, 1972.
(7) German patent application no. 102 55 363.7.

10.1021/ja037522+ CCC: $27.50

Table 1

compound	R	yield (reaction time)
2a	H	10% (1 week)
2b	*n*-C_4H_9	quant (12 h)
2c	*n*-$C_{12}H_{25}$	quant (12 h)
2d	*i*-propyl	40% (12 h)
2e	3,7-dimethyloctanyl	60% (72 h)[a]

[a] 20% conversion (^{1}H NMR) after 12 h.

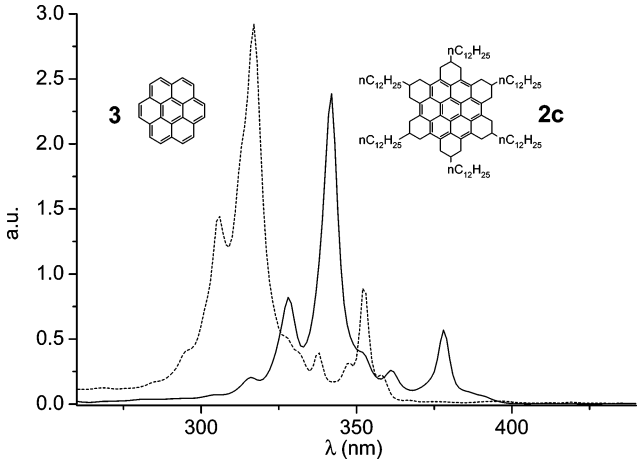

Figure 1. Absorption spectra of **2c** and coronene (THF; 10^{-4} M).

repeated heating/cooling of the filtrate to approximately 50 °C and filtration to remove residual unreacted HBC. Flash chromatography was required to separate branched-chain derivatives **2d**,**e** from residual starting materials.

Mass spectra (MALDI-TOF) indicated a single product in all cases, with isotopic distribution and nominal mass corresponding to the addition of 18 hydrogen atoms to the starting materials. Solution UV−vis absorption spectra of all derivatives match the profile of coronene, but with a bathochromic shift of 20−30 nm (Figure 1, **2c**). ^{1}H NMR spectra of compounds **2** are devoid of signals downfield from 4 ppm; that is, no protons are attached to sp^2 carbons. The ^{1}H NMR spectrum of **2a** consists of only two resonances at 3.6 (triplet, Ar***CH*$_2$**) and 2.4 (quintet, CH_2***CH*$_2$**CH_2) ppm, with ^3J (H,H) = 6.2 Hz. Only three signals arising from carbons without attached protons are present in the 110−140 ppm range of spin−echo (APT) ^{13}C spectra. ^{1}H−^{13}C correlation NMR spectra confirm the nature of the saturated alkyl periphery of those compounds (**2b**−**e**) obtained from substituted HBCs (Figure 2, compound **2b**).

Bulk Characterization. Compounds **2a** and **2b** crystallize to compact polyhedra and thin needles, so far too small for structural proof. Thermotropic behaviors of compounds **2c**,**e** were investigated by differential scanning calorimetry (DSC), polarized optical microscopy (POM), and wide-angle X-ray diffraction (WAXD). DSC thermograms obtained for both compounds are shown in Figure 3. Compound **2c** undergoes a very broad endothermic process(es) on heating (10 °C/min), beginning just below room temperature with clear maxima at 93 and 113 °C (Figure 3, curve a). The very weak, apparent second-order endotherm at approximately −30 °C (inset), as well as the endothermic maximum at 93 °C, disappear in subsequent heating scans. On cooling from above the higher endotherm, a sharp exotherm (onset 81 °C, peak 74 °C) is seen with a tail extending to below 0 °C. Cooling at a slower rate (2 °C/min, not shown) decreased the supercooling prior to this recrystallization (onset 86 °C, peak 80 °C). Optical microscopy revealed sharply defined needlelike features at lower temper-

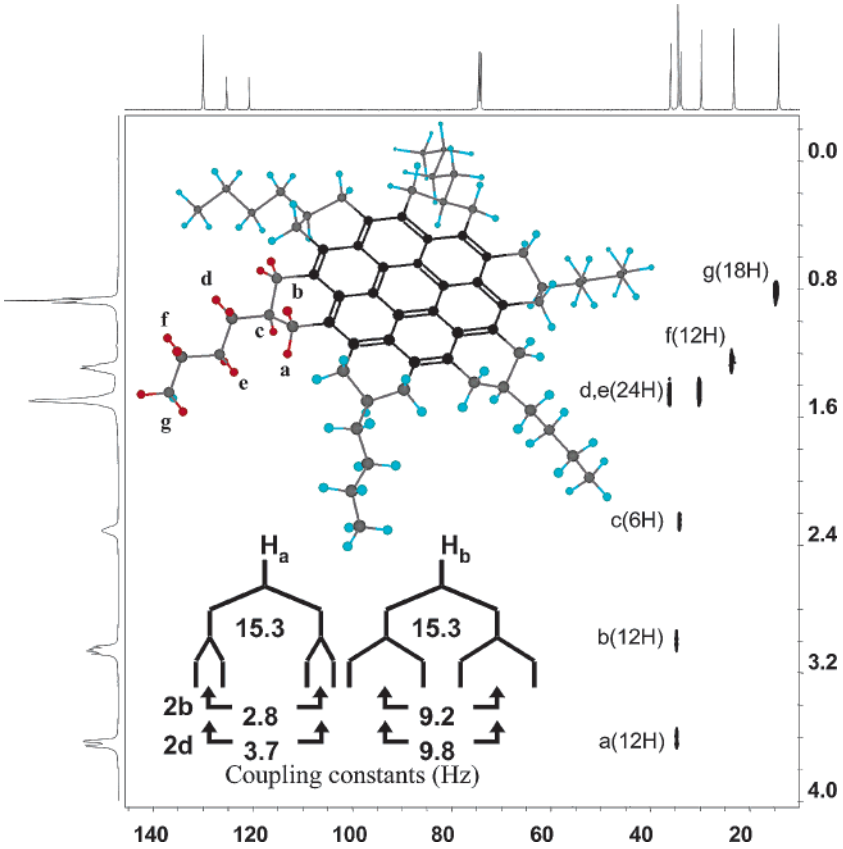

Figure 2. ^{1}H−^{13}C COSY NMR spectrum of **2b** in $C_2D_2Cl_4/CS_2$. Inset shows ^3J (H−H) splitting patterns for benzyl hydrogens of compounds **2b**,**d**.

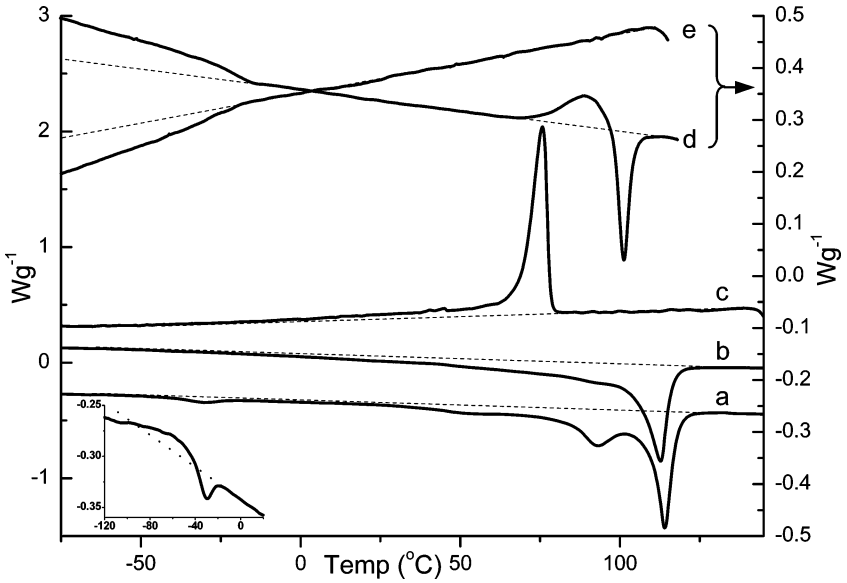

Figure 3. DSC thermograms (10 °C/min) obtained from compounds **2c**,**e**. Curves a,b,c: first heating, second heating, first cooling runs for compound **2c**. The inset is a magnification of a portion of curve a, indicating a second-order endotherm, superimposed with the beginning of continuous melting/recrystallization. Curves d,e: second heating and cooling runs for **2e**.

atures which smear out to fanlike textures upon annealing at 95 °C, suggesting an additional (meso)phase. Heating further through the transition at 113 °C results in isotropization, after which cooling produces again the needlelike textures, without the intervening optical texture seen on heating.

The second heating curve of **2e** shows a clear second-order transition (onset −27 °C, middle point −20 °C), and then a broad exotherm (peak 89 °C) just preceding a sharp endotherm (peak 101 °C). Only the second-order transition (∼ −20 °C) is observed on cooling. After the sample was annealed at 80 °C, the second-order transition is not observed in the subsequent cooling or heating scans, and the broad exotherm/endotherm is converted to a broad and highly asymmetric, but monomodal, endotherm with a maximum again at 101 °C. Optical microscopy reveals isotropization at 101 °C and no apparent birefringence on cooling to room temperature at 10 °C/min. Birefringence returns slowly (hours) when the sample is then annealed at 80 °C. Cooling of the isotropic film with a stream of cold nitrogen gas rapidly initiates the growth of sperulitic nuclei, which grow to impingement within 5 min of heating to 80 °C.

Wide-angle X-ray diffraction (WAXD) of both compounds was conducted to elucidate their mode of self-assembly. Intensity distributions obtained from representative powder measurements (reflection mode) of **2c**,**e** are shown in Figure 4. Two-dimensional WAXD measurements of aligned samples (mechanically extruded fibers)[8] were also carried out to simplify interpretation of the scattering patterns (background Figure 4, **2e**).

Charge-Carrier Mobilities. PR-TRMC was used to measure the intrinsic one-dimensional charge-carrier mobility sum ($\sum\mu_{1D}$) in compound **2c** between the temperatures of −100 and 160 °C. A plot of $\sum\mu_{1D}$ as a function of temperature is shown in Figure 5. There is a gradual increase in $\sum\mu_{1D}$ from ca. 0.4 cm^2/(V s) at the lowest temperatures up to a peak value of 0.9 cm^2/(V s) at ca. 60 °C. There is an abrupt decrease in the mobility by almost an order of magnitude upon heating above 80 °C.

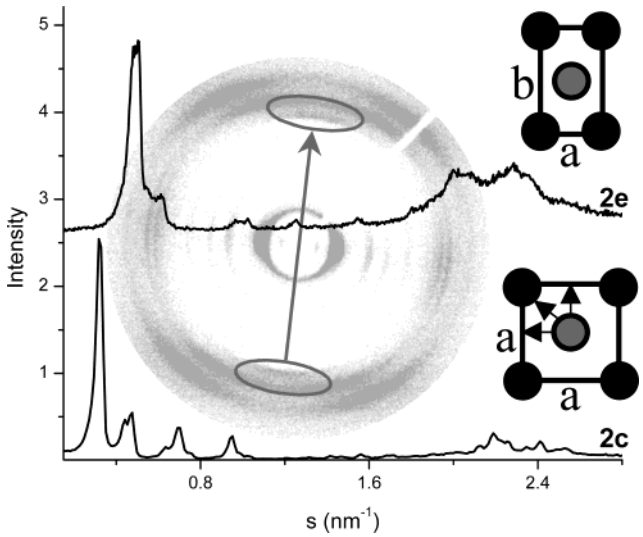

Figure 4. Wide-angle X-ray diffraction intensity distributions (powder) from **2c**,**e**. The background shows a 2D WAXS diffractogram from **2e** (oriented fiber). The arrow indicates the fiber/column direction, and elipses contain the reflexes corresponding to the stacking periodicity (d = 5.3 Å) along the columns. Unit cells are illustrated for **2e**: a = 1.95 nm, b = 3.37 nm ≈ $a\sqrt{3}$. For **2c**: a = 3.05 nm. The arrows indicate the central column is displaced from the center of cell.

Discussion

Synthesis and Structural Proof. Palladium on activated carbon catalyzes the clean conversion of *n*-alkylated HBCs to the title coronenes under relatively mild conditions (65 bar H_2, 60 °C) within 12 h. No purification is required in the cases of **2b**,**c**; the heterogeneous catalyst is simply filtered away, leaving a single detectable product in quantitative isolated yield. Passage through a short pad of silica gel with a nonpolar solvent (toluene) was sometimes necessary to remove traces of colored material. MALDI-TOF mass spectra, multinuclear NMR experiments, and UV−vis absorption spectra confirmed the structure and purity of the products.

The reaction rate is severely hindered, as judged by conversion over similar reaction times, when alkyl substituents contain

(8) Fischbach, I.; Pakula, T.; Minkin, P.; Fechtenkötter, A.; Müllen, K.; Spiess, H. W.; Saalwächter, K. *J. Phys. Chem. B.* **2002**, *106*, 6408−18.

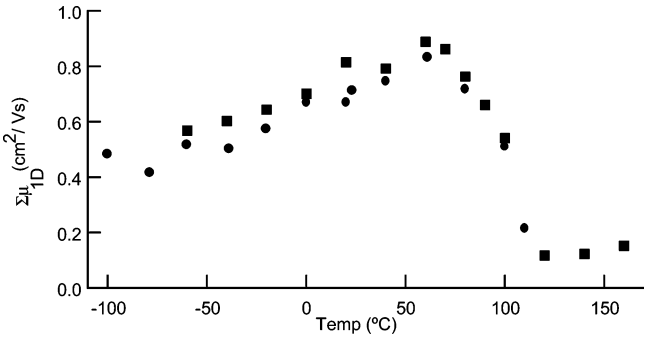

Figure 5. Variable-temperature one-dimensional sum charge-carrier mobility, $\sum\mu_{1D}$, for two independently synthesized samples of compound **2c**, measured using PR-TRMC.

an α methyl branch as in **2d** (R = *i*-prop) and even when a methyl branch is displaced to the γ position as in **2e** (Table 1). In these cases where conversion was less than quantitative, the pure coronenes could be obtained after flash chromatography through a short bed of silica gel. It is not surprising that steric bulk in the side chains hinders conversion in such a heterogeneous reaction where the disks must contact the Pd metal on the carbon surface. The fact that the somewhat distal γ methyl branches in **1e** significantly retard the reaction finds some relevance in STM studies of self-assembled, "face-on" monolayers of HBC derivatives at a solid−liquid interface. Both **1e** and its analogue carrying chiral 3,7-dimethyloctanyl chains showed notably different behavior from HBCs with *n*-alkyl chains.[9]

The solubility of unsubstituted HBC **1a** is so low that crystals suitable for X-ray analysis have so far only been grown from semidilute solution in molten pyrene.[10] However, it has recently been demonstrated[11] that self-assembled monolayers of **1a** could be formed at the solid−liquid interface between HOPG and a solvent containing **1a**. We were prompted by these observations to attempt the heterogeneous hydrogenation of **1a** and accordingly observed modest conversion over extended reaction times.

The first indication of this remarkable transformation comes from MALDI-TOF measurements where only one isotopically resolved set of signals is seen for each new coronene, corresponding to the addition of 18 hydrogen atoms to the starting HBCs. More than one possibility exists for the addition of 18 hydrogens to the HBC core, each leading to different unsaturated chromophores with varying levels of symmetry. The profiles of the solution absorption spectra of each new substituted coronene **2a**−**e** are virtually identical to that of the parent coronene (Figure 1), but red-shifted by approximately 25 nm (λ_{max} coronene, 317 nm; **2c**, 342 nm). Alkyl substitution of PAHs generally results in a red shift in the absorption spectrum, and the effect can be cumulative with increasing substitution. Hydrogenation of a dinaphthocoronene gave rise to, among other products, compounds **4** (a hexa-alkylated coronene) and **5** (a hepta-alkylated pyrene).[12] The absorption maxima of **4** are shifted by 12 nm relative to coronene, and those of **5** are shifted by ∼25 nm relative to pyrene. In the same report, **6**, produced by hydrogenation of coronene, exhibits a spectrum which is shifted by 15−18 nm relative to the parent triphenylene (Scheme 2).

Scheme 2. Highly Alkyl-Substituted PAHs

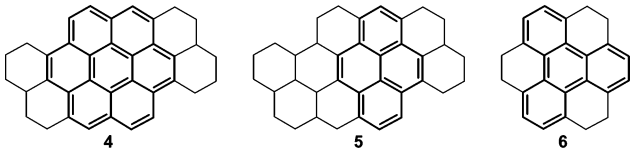

While the absorption measurements give strong indication of the proposed chromophoric core resulting from hydrogenation, more convincing structure proof comes from solution NMR measurements. The ^{1}H NMR spectrum of **2a** contains only a triplet and a quintet at 3.6 (Ar***CH*$_2$**) and 2.4 (CH_2***CH*$_2$**CH_2) ppm, respectively. The coupling constant, ^3J (H,H) = 6.2 Hz, is intermediate between those expected for axial−axial and axial−equatorial relations within conformationally rigid rings. The benzyl hydrogens are therefore equivalent, as are the homobenzyl hydrogens, suggesting rapid flipping of the peripheral rings on the NMR time scale. As for all new compounds reported here, spin−echo (APT) ^{13}C experiments showed only three signals without attached protons between 110 and 140 ppm, attributed to the aromatic quaternary carbons of persubstituted coronenes, replacing the five signals of the precursor HBCs.

The ^{1}H−^{13}C COSY spectra of the substituted derivatives are more revealing (Figure 2), particularly the ^{1}H resonances between 2 and 4 ppm, corresponding to the fused peripheral rings as indicated by lowercase letters. The inset shows the splitting patterns for protons "a" and "b", which are not equivalent due to conformational restrictions, with possible contribution from the anisotropic magnetic current. Both show a typical methylene geminal splitting to doublets (^2J (H−H) = 15.3 Hz) and are then further split to doublets by methine proton "c". H_a−H_c coupling is much weaker than H_b−H_c coupling in accordance with the Karplus relation.[13] This suggests that the alkyl chains remain in the equatorial positions; that is, the rings are not flipping on the NMR time scale at room temperature. The coupling constants are larger for R = *i*-prop (**2d**) than for *n*-butyl (**2b**), in agreement with the greater preference of bulkier groups for the equatorial position. A thorough study of the flipping of the rings as a function of temperature, as well as a function of the bulkiness of the substituents, was not undertaken after various observations[14] suggested that these disks aggregate strongly in solution, like their HBC precursors. It is expected that aggregation will also affect the ring flipping, and this cannot be decoupled from the effect of temperature and of the nature of the substituents.

The overall outcome of the hydrogenation reaction is clear, but obvious questions are raised concerning the mechanism, stereochemistry, and regiospecificity of this conversion. Pd/C favors reduction of electron-rich K-regions of PAHs, that is, areas with minimal bond delocalization energies.[15] Although all-benzenoid PAHs are described as fully delocalized π-sys-

(9) (a) Samorí, P.; Fechtenkötter, A.; Böhme, T.; Jäckel, F.; Müllen, K.; Rabe, J. P. *J. Am. Chem. Soc.* **2001**, *123*, 11462−67. (b) Tchebotareva, N.; Yin, X.; Watson, M. D.; Samorí, P.; Rabe, J. P.; Müllen, K. *J. Am. Chem. Soc.* **2003**, *125*, 9734−39.
(10) Goddard, R.; Hänel, M.; Herndon, W. C.; Krüger, C.; Zander, M. *J. Am. Chem. Soc.* **1995**, *117*, 30−41.
(11) Samorí, P.; Severin, N.; Simpson, C. D.; Müllen, K.; Rabe, J. P. *J. Am. Chem. Soc.* **2002**, *124*, 9454−57.
(12) Fromherz, H.; Thaler, L.; Wolf, G. *Z. Elektrochem.* **1943**, *49*, 387−400.
(13) Silverstein, R. M.; Bassler, C. G.; Morrill, T. C. *Spectrometric Identification of Organic Compounds*, 5th ed.; Wiley: New York, 1991; pp 208−9.
(14) Observations include increased solubility when CS_2 was added (good solvent for breaking $\pi-\pi$ contacts), significant red shift in luminescence on changing solvents and concentration, fiber formation from solution, etc.
(15) Fu, P. F.; Lee, H. M.; Harvey, R. G. *J. Org. Chem.* **1980**, *45*, 2797−2803.

tems,[6] the single-crystal molecular structure of HBC **1a** revealed that the C−C bonds in the peripheral rings are slightly shorter than those in the interior.[10] A number of theoretical studies corroborate that the "edge" benzenes of this and larger PAHs are "less aromatic" than those in the interior.[16] Although it could be a moot point here as the reaction must of course begin at the periphery, the shorter length of these bonds goes along with higher reactivity. Hydrogenation of one peripheral double bond should lead to a reduction in aromatic stabilization energy that is not compensated until the entire periphery is hydrogenated, leading to the "super-aromaticity"[17] of coronene. The fact that the reaction did not proceed further finds analogy in the Pd/C-catalyzed perhydrogenation of dodecahydrotriphenylene (a peripherally hydrogenateed all-benzenoid PAH/peralkylated benzene). Multiple unsuccessful attempts were reported before drastic conditions were used (150−200 bar, 300 °C) successfully, after which a complex balance between thermodynamic and kinetic factors was proposed.[18]

Concerning the mechanism and the related question of stereochemistry, it is probable that the disk adsorbs to the metal surface and is not released until hydrogen uptake is completed in a concerted manner. If hydrogenation is completed at a single metal site, shifting coordination from one peripheral ring to the next across "bay" regions can be imagined to take place via either η-3 allyl or η-4 butadiene coordinative complexes. It is likely that hydrogen atoms are added to only one face of the disk, but this assumption cannot be substantiated without crystallographic evidence. The solution ^{1}H NMR spectra of substituted derivatives indicate both a highly symmetric structure and that all alkyl chains are equatorial, limiting the number of reasonable stereochemical outcomes to (1) an all-cis addition of hydrogen or (2) an alternating addition of hydrogen atoms to the opposite sides of successive rings around the periphery. When D_2 is substituted for H_2 in the reduction, the three multiplets present between 2 and 4 ppm in the ^{1}H NMR spectrum of **2b** are replaced by a singlet (3.1 ppm, 12H) corresponding in chemical shift to axial benzylic protons "b" (Figure 2, protons "a" and "c" are now deuterons). However, the isotopic distribution (MALDI-TOF, Supporting Information) is somewhat extended on the high-mass side, indicating some degree of H/D exchange.

Bulk Characterization. Compounds **2a**,**b**,**d** are crystalline solids; however, to date, no single crystals large enough for single-crystal X-ray experiments could be prepared. Compounds **2b**,**d** form long thin needles,[19] while **2a** forms more compact polyhedra. Cocrystallization of **2b** with an acceptor, 2,4,7-trinitrofluoren-9-one, gave lathe-shaped crystals. This last point, cocrystallization with an acceptor or guest molecule, will receive further attention. Persubstituted coronenes (Scheme 3, **6**, X = Cl, SAr, OAr) have been investigated and shown to be effective hosts.[20] Because of steric repulsion between the substituents, the disks are nonplanar with pairs of peripheral carbons

Scheme 3. Persubstituted Coronenes

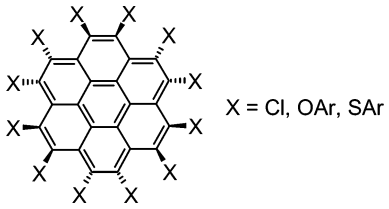

7

protruding above and below the mean plane of the molecule in a "saw-tooth" fashion. Their facility as hosts is strongly dependent on the nature of the substituents. Like nearly all such hosts based on persubstituted aromatics, the central core is surrounded by heteroatoms.[21] Compounds **2**, on the other hand, could prove to be effective, entirely hydrocarbon hosts.

The thermotropic phase behavior of compounds **2c**,**e** was studied by WAXD, POM, and DSC. The results combine to show that, despite their nonplanar periphery of puckered rings, both assemble to columnar phases in a fashion similar to that of their planar HBC precursors, albeit self-assembly is frustrated. This comparison will become particularly relevant to the understanding of one-dimensional charge transport processes along columns[22] as a function of the identity of the π-system through which the transport occurs. Few all-hydrocarbon systems exist which could be compared to HBCs in this regard.

POM shows that **2c**,**e** are birefringent below their isotropization temperatures just above 100 °C. The second heating scan (DSC, Figure 3) for compound **2c** shows a very broad endotherm (downward curvature), suggesting gradual reordering leading up to the isotropization. Two transitions present only in the first scan [second-order endotherm ($T_g \approx -35$ °C) and first-order endotherm (melting ~94 °C)] indicate disordered/poorly ordered states produced during isolation of the material. The first heating scan for **2e** shows similar features.[23] However, while **2c** shows a typical melting/reassembly hysteresis (~30 °C), molten **2e** supercools to a glass at −20 °C, indicated by the reversible second-order transition in Figure 3. Self-assembly then occurs on heating, as indicated by the first-order exotherm just prior to isotropization. No birefringence is seen under cross polarizers over long periods of time if the isotropic melt is cooled only to room temperature. Cooling a sample just prior to complete isotropization (few small birefringent spots remaining) results in relatively fast "recrystallization".[24] Nucleation is the rate-limiting step here and does not occur or is relatively slow at room temperature. Polymorphism (coexistence of two phases of differing order) is clearly present at room temperature after specific thermal treatments.[23] Annealing a sample in the differential scanning calorimeter at 89 °C eliminates the glass transition and the exothermic "recrystallization" on subsequent

(16) Moran, D.; Stahl, F.; Bettinger, H. F.; Schäfer, H. F., III; Schleyer, P. v. R. *J. Am. Chem. Soc.* **2003**, *125*, 6746−52.
(17) Zhou, Z. X. *J. Phys. Org. Chem.* **1995**, *8*, 103−07.
(18) Farina, M. *Tetrahedron Lett.* **1963**, 2097−2100. Farina, M.; Di Silvestro, G.; Sozzani, P. In *Comprehensive Supramolecular Chemistry*; Atwood, J. L., Davies, J. E. D., Macnicol, D. D., Vögtle, F., Eds.; Pergamon Press: Oxford, 1996; Vol. 6, Chapter 12.
(19) Much like their precursors, a common problem with substituted discotic molecules. See, for example: Bushby, R. J.; Boden, N.; Kilner, C. A.; Lozman, O. R.; Lu, Z.; Quanying, L.; Thornton-Pett, M. A. *J. Mater. Chem.* **2003**, *13*, 470−74.
(20) Baird, T.; Gall, J. H.; Macnicol, D. D.; Mallinson, P. R.; Michie, C. R. *J. Chem. Soc., Chem. Commun.* **1988**, 1471−73. Frampton, C. S.; MacNicol, D. D.; Rowan, S. J. *J. Mol. Struct.* **1997**, *405*, 169−78. Shibata, K.; Kulkarni, A. A.; Ho, D. M.; Pascal, R. A., Jr. *J. Org. Chem.* **1995**, *60*, 428−34. Downing, G. A.; Frampton, C. S.; MacNicol, D. D.; Mallinson, P. R. *Angew. Chem., Int. Ed. Engl.* **1994**, *33*, 1587−89.
(21) Macnicol, D. D.; Downing, G. A. In *Comprehensive Supramolecular Chemistry*; Atwood, J. L., Davies, J. E. D., Macnicol, D. D., Vögtle, F., Eds.; Pergamon Press: Oxford, 1996; Vol. 6, Chapter 14.
(22) van de Craats, A. M.; Warman, J. M. *Adv. Mater.* **2001**, *13*, 130−33.
(23) Supporting Information.
(24) Similar to other discotics, WAXD measurements indicate that the rigid molecular cores are "crystallized" at room temperature but the side chains may be liquidlike or partially crystallized. The room temperature phases may be plastically deformed to give aligned, optically clear films/fibers.

scans (not shown), indicating conversion of the isotropic material to the columnar phase.

The thermal behaviors of **2c**,**e** are dramatically different from their planar precursors. The isotropization temperatures are ~300 °C lower[25] in both cases, probably due to decreased intracolumnar stabilization associated with a smaller π-system and to increased steric interference by the puckered-ring periphery at higher temperatures. Reassembly is frustrated (hysteresis) by the molecular shape, and this effect is magnified by the γ-branches within the side chains of **2e**. A low melting temperature is, however, advantageous as it can allow thermal processing to increase purity and to direct columnar alignment.[26]

Temperature-dependent WAXD measurements show that, despite inhibition of the initial assembly, compounds **2c**,**e** do pack into ordered columnar structure(s) (Figure 4). 2D WAXD diffractograms from aligned samples consist of three sets of features: (1) a set of arcs along the equator describing lateral columnar packing, (2) a symmetric, hyperbolic set of reflections with vertexes centered on the meridian at a position giving the intracolumnar stacking distance, and (3) a diffuse halo resulting from the liquidlike correlation of alkyl side chains. For both **2c**,**e**, arcs on the meridian occur with a *d* spacing of ~5.3 Å. Such a large deviation from the normal van der Waals stacking distance (~3.5 Å) of PAHs would be expected to have a large negative effect on bulk charge-carrier mobility,[27] contrary to what is reported here. Generally, discotics based on PAH molecules tilt relative to the columnar axes when in their lower temperature "crystalline" phases, and for the parent HBCs **1c**,**e**, this tilt is approximately 45−50°.[28] Assuming that the periphery of these peralkylated coronenes does not dramatically change the normal van der Waals stacking distance (~3.5 Å), their tilt angle can be calculated as $\phi = \arccos(3.5\ \text{Å}/5.3\ \text{Å}) = 49°$.

The equatorial intensity distributions from the room-temperature WAXD diffractograms were fit to the 2D unit cells included in Figure 4. The columnar packing of **2e** is essentially the same as that for its precursor,[28] pseudohexagonal (orthorhombic with $b = a\sqrt{3}$). Even though the disks are tilted (45−50°), giving them an elliptical cross section, the achiral branched side chains most likely remain completely fluid and compensate to maintain an overall cylindrical shape. For compound **2c**, 10 of the first 13 reflexes at room temperature can be reasonably well fit to columns arranged in a 2D square lattice ($a = 3.05$ nm) and with intercolumnar distances of 2.15 nm. The arrows in the unit cell indicate that the central column is most likely displaced from the center, such that the [100]/[010] reflex is not extinguished. Heating both samples below their isotropization results in a progressive sharpening and increase in the number of the reflexes, indicating increased order and a change in symmetry, corresponding to slight changes seen by POM and to the nonlinear DSC baseline. No attempt was made to assign these transient phases.

Charge-Carrier Mobilities. The high charge-carrier mobilities measured for the derivative **2c** are comparable to those obtained previously in HBC derivatives with C10, C12, C14, and phenyl-C12 side chains.[29] The half-life for the charge carriers is ca. 5 μs in the crystalline phase at room temperature, which is about 3 times as long as the best of the HBC derivatives indicated above. This may be explained by the increased saturated hydrocarbon region immediately surrounding the aromatic core, that is, 18 sp^3 carbon atoms rather than 6 in **1c**. This provides a larger barrier toward charge recombination via intercolumnar tunneling.

Concluding Remarks

We have presented a remarkable chemical transformation, the regiospecific hydrogenation of all-benzenoid π-systems (hexa-*peri*-hexabenzocoronenes) to novel circumarenes, the first peralkylated coronenes. Strong indications of an all-syn addition of hydrogen atoms come from solution NMR experiments. The saturated periphery frustrates nucleation, but does not preclude assembly to highly ordered columnar structures via $\pi-\pi$ stacking, and in fact could enhance order by some interlocking. Currently, we are investigating self-assembly from solution; for example, compound **2c** forms a network of long fibers, sufficient to gel the mother liquor, similar to the precursor HBC **1c**.[30] Both the high mobility and the long lifetimes of the charge carriers bode favorably for their use in molecular electronics. Coupled with their intrinsic charge-carrier characteristics, their relative ease of synthesis and processibility can also be advantageous in the fabrication of useful devices. Ongoing work includes evaluation of these molecules as hosts and expanding the scope of this selective reduction to include other all-benzenoid PAHs of various size and shape. We have already observed the conversion of a homologue with 60 core carbons[31] to the first peralkylated circumbiphenyl.[32] Last, these molecules offer the promise of new functional materials with varied electron/hole transporting properties following functionalization of the newly formed "benzylic" positions.

Acknowledgment. This work was financially supported in part by the Zentrum für Multifunktionelle Werkstoffe und Miniaturisierte Funktionseinheiten (BMBF 03N 6500), EU-TMR project SISITOMAS, the Deutsche Forschungsgemeinschaft (Schwerpunkt Feldeffecttransistoren), and the EU project DISCEL (G5RD-CT-2000-00321).

Supporting Information Available: Full experimental details, optical micrograph and DSC trace of compound **2e**, and MALDI-TOF spectra (PDF). This material is available free of charge via the Internet at http://pubs.acs.org.

JA037522+

(25) Fechtenkötter, A.; Tchebotareva, N.; Watson, K.; Müllen, K. *Tetrahedron* **2001**, *57*, 3769−3783 and references therein.
(26) Liu, C.-Y.; Bard, A. J. *Chem. Mater.* **2000**, *12*, 2353−62. Cooling of isotropic thin films along a heat gradient or on Teflon alignment layers results in alignment of columns parallel to the surface as indicated by POM.
(27) Liu, C.-Y.; Bard, A. J. *Nature* **2002**, *418*, 162−64.
(28) (a) Bunk, O.; Nielsen, M. M.; Sølling, T. I.; van de Craats, A. M.; Stutzmann, N. *J. Am. Chem. Soc.* **2003**, *125*, 2252−58. (b) van de Craats, A. M.; Stutzmann, N.; Bunk, O.; Nielsen, M. M.; Watson, M. D.; Müllen, K.; Chanzy, H. D.; Sirringhaus, H.; Friend, R. H. *Adv. Mater.* **2003**, *15*, 495−99.
(29) van de Craats, A. M.; Warman, J. M.; Fechtenkötter, A.; Brand, J. D.; Harbison, M. A.; Müllen, K. *Adv. Mater.* **1999**, *11*, 1469−1472.
(30) Tracz, A.; Wostek, D.; Kucinska, I.; Jeszka, J. K.; Watson, M.; Müllen, K.; Pakula, T. In *NATO ASI Series*; Graja, A., Bulka, B. R., Kajzar, F., Eds.; Kluwer Academic Publishers: Dordrecht, 2002; pp 315−318.
(31) Iyer, V. S.; Yoshimura, K.; Enkelmann, V.; Epsch, R.; Rabe, J. P.; Müllen, K. *Angew. Chem., Int. Ed.* **1998**, *37*, 2696−99.
(32) Simpson, C. D. Nanoscale Polycyclic Aromatic Hydrocarbons-Synthesis and Characterization. Ph.D. Dissertation, Johannes Gutenberg University, Mainz, 2003.